Mineralogical Magazine (2023), 1–5
doi:10.1180/mgm.2023.56

CAMBRIDGE UNIVERSITY PRESS

Article

Minerals with a palmierite-type structure. Part II. Nomenclature and classification of the palmierite supergroup.

Rafał Juroszek[1], Biljana Krüger[2], Hannes Krüger[2] and Irina Galuskina[1]

[1]Institute of Earth Sciences, Faculty of Natural Sciences, University of Silesia, Będzińska 60, 41-205, Sosnowiec, Poland; and [2]Institute of Mineralogy and Petrography, University of Innsbruck, Innrain 52, 6020, Innsbruck, Austria

Abstract

The palmierite supergroup, approved by the IMA-CNMNC, includes five mineral species characterised by the general crystal-chemical formula $^{XII}M1^{X}M2_2(^{IV}TO_4)_2$ ($Z = 3$). On the basis of the crystal-chemical arguments and heterovalent isomorphic substitution scheme $M^{+}+T^{6+} \leftrightarrow M^{2+}+T^{5+}$, the palmierite supergroup can be formally divided into two groups: the palmierite group $M1^{2+}M2_2^{+}(T^{6+}O_4)_2$, and the tuite group $M1^{2+}M2_2^{2+}(T^{5+}O_4)_2$. Currently, the palmierite group includes palmierite $K_2Pb(SO_4)_2$, and kalistrontite $K_2Sr(SO_4)_2$, whereas the tuite group combines tuite $Ca_3(PO_4)_2$, mazorite $Ba_3(PO_4)_2$, and gurimite $Ba_3(VO_4)_2$. The isostructural supergroup members crystallise in space group $R\bar{3}m$ (no. 166). The palmierite-type crystal structure is characterised by a sheet arrangement composed of layers formed by $M1O_{12}$ and $M2O_{10}$ polyhedra separated by TO_4 tetrahedra perpendicular to the *c* axis. The abundance of distinct ions, which may be hosted at the *M* and *T* sites (*M* = K, Na, Ca, Sr, Ba, Sr, Pb, Rb, Zn, Tl, Cs, Bi, NH_4 and REE; *T* = Si, P, V, As, S, Se, Mo, Cr and W) implies many possible combinations, resulting in potentially new mineral species. Minerals belonging to the palmierite supergroup are relatively rare and usually form under specific conditions, and their synthetic counterparts play a significant role in various industrial applications.

Keywords: palmierite supergroup; palmierite group; tuite group; palmierite; kalistrontite; tuite; gurimite; mazorite; mineral nomenclature

(Received 5 June 2023; accepted 17 July 2023; Accepted Manuscript published online: 24 July 2023; Associate Editor: Oleg I Siidra)

Introduction

The palmierite-type structure is characteristic of a wide group of compounds that includes minerals and synthetic materials (Zachariasen, 1948; Süsse and Buerger, 1970; Sugiyama and Tokonami, 1990; Tissot *et al.*, 2001; Thompson *et al.*, 2013; Tsyrenova *et al.*, 2016; Bismayer *et al.*, 2017; Kemp *et al.*, 2018). In the literature on synthetic compounds with the palmierite-type structure, the general formula is presented in two different ways: $M_3(TO_4)_2$ (Grzechnik and McMillan, 1997; Thompson *et al.*, 2013) and $M1M2_2(TO_4)_2$ (Moore, 1973; Tsyrenova *et al.*, 2016), where $M = Ba^{2+}$, Sr^{2+}, Ca^{2+}, Pb^{2+}, Rb^{+}, K^{+}, Na^{+}, NH_4^{+}, Tl^{+} and REE^{3+}, and $T = V^{5+}$, As^{5+}, P^{5+}, S^{6+}, Cr^{6+}, Se^{6+}, Mo^{6+} and W^{6+}. Moreover, this type of structure is also noted for materials with the formula $A_5R(MoO_4)_4$ (A^{+} = K, Rb and Tl; R^{3+} = REE, Y, Bi, Fe and In)(Tsyrenova *et al.*, 2016). Currently, the inorganic crystal structure database (ICSD, https://icsd.products.fiz-karlsruhe.de/) lists ~100 compounds with the same structure type and, depending on the chemical composition, these palmierite-type materials exhibit various optical, luminescence, ferroelectric and catalytic properties (Lagos, 1970; Grzechnik and McMillan, 1997; Mugavero *et al.*, 2008; Thompson *et al.*, 2013; Tong *et al.*, 2015). Some compounds, due to the crystal structure flexibility, can accommodate large ion lithophile elements (LILE) and different luminescent ions, mainly rare-earth elements (REE) (Lagos, 1970; Murayama *et al.*, 1986; Sugiyama and Tokonami, 1987; Xie *et al.*, 2004; Thompson *et al.*, 2013; Cao *et al.*, 2014; Tong *et al.*, 2015).

Most palmierite-type materials, mainly high-temperature compounds, are trigonal (usually described in a rhombohedral unit cell), isostructural and crystallise in space group $R\bar{3}m$ (no. 166). The crystal structure comprises two non-equivalent *M*-cation sites and a tetrahedrally coordinated *T* site, which form a three-dimensional anionic framework (Moore, 1973; Sugiyama and Tokonami, 1987; Azdouz *et al.*, 2010). However, there are a few monoclinic compounds with *C*2/*c* space group, mainly molybdates (Tsyrenova *et al.*, 2016). The symmetry reduction (transition) from trigonal to monoclinic is related to the structure distortion, mostly noticed through the shifts of *M*-cations and $(PO_4)^{3-}$ anions from the special position on three-fold axes (Tsyrenova *et al.*, 2016).

The present work describes the nomenclature and classification of the palmierite supergroup approved by the Commission on New Minerals, Nomenclature and Classification of the International Mineralogical Association (IMA-CNMNC Proposal 22-L, Bosi *et al.*, 2023). The proposal to the IMA and the requirement for developing the palmierite supergroup classification are related to the discovery of a new mineral, mazorite $Ba_3(PO_4)_2$ (IMA2022–022; Juroszek *et al.*, 2023). The approval of the nomenclature and the classification of the palmierite supergroup allows us to not only classify the five minerals into one structural supergroup, but also to formally use the name already firmly established in the literature.

Corresponding author: Rafał Juroszek; Email: rafal.juroszek@us.edu.pl
Cite this article: Juroszek R., Krüger B., Krüger H. and Galuskina I. (2023) Minerals with a palmierite-type structure. Part II. Nomenclature and classification of the palmierite supergroup.. *Mineralogical Magazine* 1–5. https://doi.org/10.1180/mgm.2023.56

Nomenclature and classification of the palmierite supergroup

The general crystal-chemical formula for the palmierite-supergroup minerals is $^{XII}M1^{X}M2_2(^{IV}TO_4)_2$ ($Z = 3$), where the left superscripts (Roman numerals) indicate the ideal coordination numbers. The M sites can be occupied by K, Na, Ca, Sr, Ba, Sr, Pb, Rb, Zn, Tl, Cs, Bi, NH_4 and REE with 1+, 2+ and 3+ charges. In turn, the T site can be occupied by Si, P, V, As, S, Se, Mo, Cr and W with 4+, 5+ and 6+ charges. The palmierite supergroup includes five mineral species, defined chemically as sulfates, phosphates and vanadates (Table 1). According to the data on synthetic analogues and their structure type, this supergroup may also include chromates, molybdates, selenates, arsenates and wolframates (Morris *et al.*, 1977; Chance and Loye, 2013; Tsyrenova *et al.*, 2016; Bismayer *et al.*, 2017; Smith *et al.*, 2020).

The heterovalent isomorphic substitution scheme $M^{+}+T^{6+} \leftrightarrow M^{2+}+T^{5+}$ implies many possible combinations of different ions and, thus, of potentially new mineral species in the palmierite supergroup. Moreover, such a scheme allows us to distinguish two groups on the basis of crystal-chemical arguments: the palmierite group $M1^{2+}M2_2^{+}(T^{6+}O_4)_2$ for the sulfates; and the tuite group $M1^{2+}M2_2^{2+}(T^{5+}O_4)_2$ for phosphates/vanadates. At this moment, the palmierite supergroup includes five mineral species: palmierite $K_2Pb(SO_4)_2$, kalistrontite $K_2Sr(SO_4)_2$, tuite $Ca_3(PO_4)_2$, gurimite $Ba_3(VO_4)_2$ and mazorite $Ba_3(PO_4)_2$.

According to the IMA-CNMNC rules (Mills *et al.*, 2009), the name of the established mineral supergroup should originate from palmierite, which was described as the first mineral species in this supergroup (Lacroix, 1907; Zambonini, 1921). Moreover, the term 'palmierite-type structure' is commonly used within the literature on various synthetic compounds (Thompson *et al.*, 2013; Tsyrenova *et al.*, 2016; Bismayer *et al.*, 2017).

Background information of the palmierite-supergroup members

Palmierite group:

Palmierite $K_2Pb(SO_4)_2$, is a rare fumarolic mineral that occurs as a result of volcanic eruptions, described for the first time by Lacroix (1907) at Mount Vesuvius in Italy. Using synthetic crystals, Zambonini (1921) performed more detailed analyses and redefined the composition of palmierite. The same material was also used for microscopic and X-ray studies (Bellanca, 1946). Later, palmierite was synthesised using thermal and aqueous methods (von Schwarz, 1966). Morris *et al.* (1977) and Tissot *et al.* (2001) obtained the experimental powder X-ray diffraction patterns. To the best of our knowledge, there is no structural data for natural palmierite. As a rare mineral, palmierite has been found in only a few localities around the world. At the Satsuma-Iwojima volcano in Japan, it occurs as a natural fumarolic sublimate (Africano *et al.*, 2002). At the Tolbachik volcano (Kamchatka Peninsula, Russia), it was detected in association with the new mineral cupromolybdite $Cu_3O(MoO_4)_2$ (Zelenski *et al.*, 2012).

Kalistrontite $K_2Sr(SO_4)_2$, the Sr-analogue of palmierite, was first described from the Lower Permian evaporites near the village of Alshtan in Bashkiria, Russia, where it formed as a result of the reaction of sylvite from anhydrite layers with Sr-bearing solutions (Voronova, 1962). Worldwide occurrences of kalistrontite are related to the Permo–Triassic, Neogene, or younger sedimentary evaporite deposits in Germany, Ukraine, China, Namibia, Israel and Turkey (Bader and Boehm, 1966; Griniv *et al.*, 1986; Min, 1987; Mees, 1999; García-Veigas *et al.*, 2009, 2011). In contrast to the mentioned localities, in Italy kalistrontite occurs within the Pleistocene geothermal field at Latium (Maras, 1979). Kalistrontite usually forms due to alteration of primary evaporite minerals or as an early diagenetic precipitate from high K- and SO_4-rich brines (Kemp *et al.*, 2018). Except for the first description, the most detailed mineralogical characterisation of kalistrontite was done on a sample from the Permian polyhalite-bearing evaporite deposits in North Yorkshire, UK (Kemp *et al.*, 2018). These authors provided results of the structure analyses from powder X-ray diffraction, as well as chemical, thermal and isotopic data. Moreover, the Raman spectrum of kalistrontite was presented in this work for the first time.

Tuite group:

Tuite γ-$Ca_3(PO_4)_2$, is a high-pressure polymorph of β-$Ca_3(PO_4)_2$ (Xie *et al.*, 2004). The transition from the β to γ phase occurs at 1000°C and 25 GPa (Murayama *et al.*, 1986). Additionally, two more polymorphs of $Ca_3(PO_4)_2$ exist, α and α′, which are stable

Table 1. Minerals of the palmierite supergroup and their synthetic counterparts.

Mineral name		Ideal formula	Space group	*a* (Å)	*c* (Å)	*V* (Å^3)	*Z*	Reference
Palmierite	synthetic	$K_2Pb(SO_4)_2$	$R\bar{3}m$	5.4950(6)	20.849(4)	545.18	3	Morris *et al.* (1977)
	synthetic		$R\bar{3}m$	5.497(1)	20.861(3)	545.8(5)	3	Tissot *et al.* (2001)
Kalistrontite	natural	$K_2Sr(SO_4)_2$	$R\bar{3}m$	5.45(3)	20.7(1)	532	3	Voronova (1962)
	natural		$R\bar{3}m$	5.45826(5)	20.8118(2)	536.968(3)	3	Kemp *et al.* (2018)
	synthetic		$R\bar{3}m$	5.4630(3)	20.843(1)	538.73	3	Morris *et al.* (1977)
Tuite	natural	$Ca_3(PO_4)_2$	$R\bar{3}m$	5.258(1)	18.727(3)	448.3(6)	3	Xie *et al.* (2002, 2004)
	synthetic		$R\bar{3}m$	5.2487(6)	18.6735(36)	445.5(1)	3	Sugiyama and Tokonami (1987)
	synthetic		$R\bar{3}m$	5.2576(2)	18.7049(13)	447.7(6)	3	Xie *et al.* (2002)
	synthetic		$R\bar{3}m$	5.2587(10)	18.691(4)	447.6(2)	3	Zhai *et al.* (2013)
	synthetic		$R\bar{3}m$	5.2522(9)	18.690(3)	446.5(2)	3	Thompson *et al.* (2013)
Gurimite	natural	$Ba_3(VO_4)_2$	$R\bar{3}m$	5.784(1)	21.132(1)	612.2(2)	3	Galuskina *et al.* (2017)
	natural		$R\bar{3}m$	5.71860(10)	21.2436(4)	601.642(19)	3	Juroszek *et al.* (2023)
	synthetic		$R\bar{3}m$	5.762(8)	21.29(3)	612.3	3	Süsse and Buerger (1970)
	synthetic		$R\bar{3}m$	5.7845(2)	21.317(1)	617.73	3	Morris *et al.* (1977)
	synthetic		$R\bar{3}m$	5.7733(14)	21.339(10)	615.961	3	Mugavero *et al.* (2008)
Mazorite	natural	$Ba_3(PO_4)_2$	$R\bar{3}m$	5.6617(5)	21.1696(17)	587.68(9)	3	Juroszek *et al.* (2023)
	synthetic		$R\bar{3}m$	5.6038(7)	21.000(5)	571.1(1)	3	Sugiyama and Tokonami (1990)

https://doi.org/10.1180/mgm.2023.56 Published online by Cambridge University Press

at high-temperature conditions (Sugiyama and Tokonami, 1987; Xie *et al.*, 2004; Thompson *et al.*, 2013; Zhai *et al.*, 2013). The γ-$Ca_3(PO_4)_2$ phase was first obtained as a product of apatite decomposition (Murayama *et al.*, 1986), and such a process is usually used to obtain tuite in synthesis experiments (Zhai *et al.*, 2013). Natural tuite was discovered in association with ringwoodite, majorite and hollandite in a shocked vein of the Suizhou L6 chondrite (Xie *et al.*, 2002, 2004). Its formation conditions were specified to be up to 23 GPa and 2000°C (Xie *et al.*, 2004). So far, tuite has been detected only in extraterrestrial rock samples (meteorites). The γ-$Ca_3(PO_4)_2$ phase, due to the crystal structure and the presence of large, high-coordination cation sites, can accommodate REE and LILE elements, such as Sr and Ba, under *P*–*T* conditions of the upper mantle (Murayama *et al.*, 1986; Sugiyama and Tokonami, 1987; Xie *et al.*, 2004; Zhai *et al.*, 2013; Skelton and Walker, 2017).

Gurimite $Ba_3(VO_4)_2$, is an alkaline earth metal orthovanadate found only in natural outcrops in the pyrometamorphic rock of the Hatrurim Complex in Israel (Galuskina *et al.*, 2017; Krzątała *et al.*, 2020). Its formation is related to the crystallisation from residual melt enriched in incompatible elements that fill interstices between the main rock-forming minerals of paralava (Galuskina *et al.*, 2017). The crystal structure of synthetic Ba orthovanadate was investigated in detail (Süsse and Buerger, 1970; Morris *et al.*, 1977; Mugavero *et al.*, 2008; Azdouz *et al.*, 2010), whereas for its natural counterpart enriched in P^{5+}, the single-crystal X-ray diffraction investigation was carried out only recently (Juroszek *et al.*, 2023). Previously, only electron back-scatter diffraction (EBSD) data were available (Galuskina *et al.*, 2017). Synthetic $Ba_3(VO_4)_2$ and their Sr-analogue have been analysed extensively due to their optical and ferroelectric properties, which indicated that such compounds could be used as luminophores, host material for lasers or television tubes (Merkle *et al.*, 1992; Grzechnik and McMillan, 1997; Mugavero *et al.*, 2008; Azdouz *et al.*, 2010).

Mazorite $Ba_3(PO_4)_2$, the P-analogue of gurimite, is a new mineral that was recently found as an accessory phase in coarse-grained gehlenite–rankinite paralava in the Hatrurim Complex

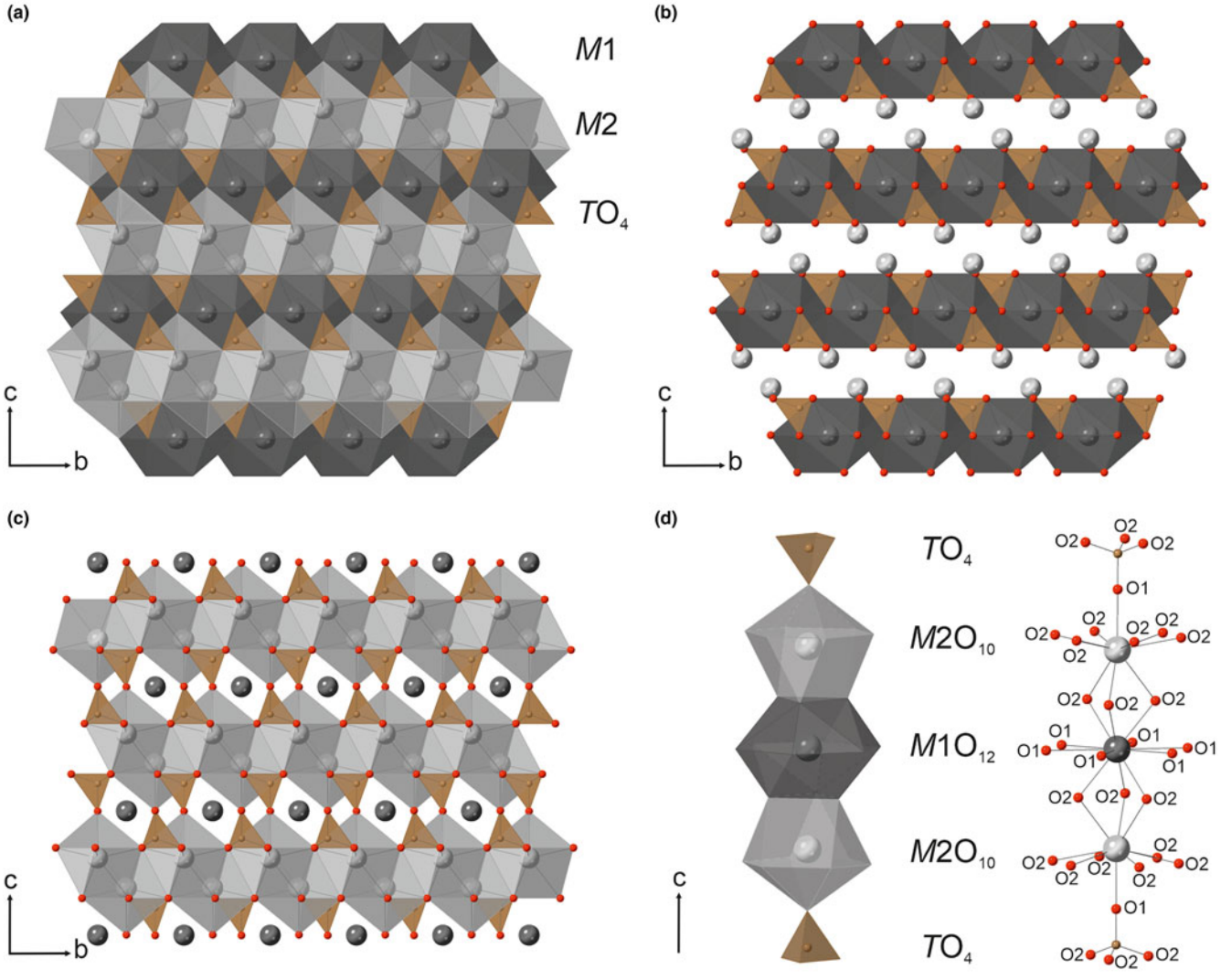

Figure 1. (a) The general view of the palmierite-type structure along (010) consists of a three-dimensional framework constructed of cations at *M*1, *M*2 and *T* sites. (b) The $M1O_{12}$ polyhedra are linked by edges to each other and form layers along (010). (c) The $M2O_{10}$ polyhedra share square faces and corners and form a layer arrangement along the *b* axis. (d) The interconnected polyhedral sequence TO_4–$M2O_{10}$–$M1O_{12}$–$M2O_{10}$–TO_4 present in the palmierite-type structure and the linkage scheme of polyhedral cations and surrounded oxygen atoms.

https://doi.org/10.1180/mgm.2023.56 Published online by Cambridge University Press

in Israel (IMA2022–022; Juroszek *et al.*, 2023). The similarity of crystallisation conditions between mazorite and gurimite, as well as the relationship with the associated Ba-bearing minerals like celsian, hexacelsian, walstromite, fresnoite, zadovite and barioferrite, in both cases, confirm the high-temperature formation of this phase. Moreover, mazorite was also detected in a carbonate–silicate xenolith from the Bellerberg volcano area in Germany, where it occurs as a small inclusion (<15 μm) inside the bennesherite crystal (Juroszek and Ternes, 2022). Synthetic mazorite doped with various metals and rare earth elements is an important phosphor material characterised by colour purity and good luminescence efficiency (Tāle *et al.*, 1979; Mu and He, 2012; Tong *et al.*, 2015).

Crystal structure of palmierite-supergroup minerals

Minerals and synthetic compounds with the palmierite-type structure crystallise in space group $R\bar{3}m$ (no. 166) (Table 1). Generally, the crystal structure of the palmierite-supergroup minerals consists of a three-dimensional framework constructed of cations at *M*1, *M*2 and *T* sites (Fig. 1a). Two large metal and symmetrically non-equivalent *M* sites are distinguished within the palmierite-type structure. The *M*1 atom, located at a 3*a* Wyckoff position with $\bar{3}m$ site symmetry, is coordinated by twelve oxygen atoms. These $M1O_{12}$ polyhedra are linked by edges to each other and form layers perpendicular to *c* (Fig. 1b). In turn, the *M*2 atom placed at a 6*m* Wyckoff position with 3*m* point symmetry is ten-coordinated. The $M2O_{10}$ polyhedra share square faces and corners and form layers perpendicular to *c* (Fig. 1c). The *T* atom in the palmierite-type structure is tetrahedrally coordinated by oxygen atoms. The TO_4 tetrahedra share edges and corners with $M1O_{12}$ and $M2O_{10}$ polyhedra (Fig. 1a–c).

A characteristic feature of the palmierite-type structure is the translationally interconnected sequence of polyhedra TO_4–$M2O_{10}$–$M1O_{12}$–$M2O_{10}$–TO_4 along the direction of the *c* axis (Fig. 1d) (Moore, 1973; Sugiyama and Tokonami, 1987). This so-called 'columnar arrangement' shows that the $M1O_{12}$ polyhedron shares two triangular faces, formed via O2 oxygen atoms from both sides, with two $M2O_{10}$ polyhedra (up and down). The remaining six O1 atoms are located in the same plane around *M*1. It should be emphasised that the six *M*1–O1 bond lengths are notably longer than the other six *M*1–O2 bonds (Fig. 1d). In the $M2O_{10}$ polyhedra, the six *M*2–O2 bonds form a hexagonal arrangement in the plane around the *M*2 atom, three *M*2–O2 derive from the triangular faces shared with $M1O_{12}$ polyhedra, and one *M*2–O1 is a bridging oxygen between $M2O_{10}$ polyhedra and TO_4 tetrahedra (Fig. 1d). The TO_4 tetrahedra show one shorter *T*–O1 and three longer *T*–O2 bond lengths.

Comment on the palmierite supergroup

Minerals of the palmierite supergroup with the approved general crystal-chemical formula $^{XII}M1^{X}M2_2(^{IV}TO_4)_2$ are divided into two groups based mainly on the heterovalent isomorphic substitution scheme $M^{+}+T^{6+} \leftrightarrow M^{2+}+T^{5+}$. The palmierite group $M1^{2+}M2_2^{+}(T^{6+}O_4)_2$ includes trigonal sulfates, which contain different prevailing (species-defining) cations at the *M*1 and *M*2 sites. In turn, the tuite group $M1^{2+}M2_2^{2+}(T^{5+}O_4)_2$ comprises trigonal phosphates and vanadates characterised by the same prevailing (species-defining) cations at both the *M*1 and *M*2 sites. The overall cation charge based on possible cation site occupancies equals 16 in both groups. However, there is no principle rule concerning the occupation of these sites by specific cations. This may trigger problems determining the crystal-chemical formulae of possible new supergroup members. The following cations, S^{6+}, Mo^{6+}, Cr^{6+}, Se^{6+}, W^{6+}, P^{5+}, V^{5+}, As^{5+} and Si^{4+}, are expected to be allocated at the tetrahedrally coordinated *T* site. All remaining cations will occupy the polyhedral *M* sites. According to the general crystal-chemical consideration and relation to other mineral supergroups, e.g. the apatite supergroup (Pasero *et al.*, 2010), we assume that the *M* sites will be filled with cations in order of increasing ionic radius, with smaller cations such as Ca^{2+} at the *M*1 site, and larger cations such us Ba^{2+} and K^{+} at the *M*2 site. This assumption is valid for the members of the palmierite group. In the tuite group, the same cation may occupy both *M* sites. This indicates that the precise evaluation of the electron density at each site is required, and a structural investigation should be mandatory.

To summarise, there is a need to perform a structural study of potential new members of the palmierite supergroup because the abundance of different ions, which may be hosted primarily at the *M*1, *M*2, and also *T* crystal sites, and the isostructural relation between the natural samples and synthetic materials, suggests that many more minerals and isomorphic series could exist within this supergroup.

Acknowledgements. The authors thank three anonymous reviewers for their helpful and constructive comments, which allowed them to improve a previous version of the manuscript.

Competing interests. The authors declare none.

References

Africano F., Van Rompaey G., Bernard A. and Le Guern F. (2002) Deposition of trace elements from high temperature gases of Satsuma-Iwojima volcano. *Earth, Planets and Space*, **54**, 275–286.

Azdouz M., Manoun B., Essehli R., Azrour M., Bih L., Benmokhtar S., Hou A. and Lazor P. (2010) Crystal chemistry, Rietveld refinements and Raman spectroscopy studies of the new solid solution series: $Ba_{3-x}Sr_x(VO_4)_2$ ($0 \leq x \leq 3$). *Journal of Alloys and Compounds*, **498**, 42–51.

Bader E. and Boehm G. (1966) Kalistrontite in the Stassfurt seam of the Rossleben-Unstrut district. *Chemie der Erde*, **25**, 253–257.

Bellanca A. (1946) La struttura della palmierite. *Periodico di Mineralogia*, **15**, 5–25.

Bismayer U., Mihailova B. and Angel R. (2017) Ferroelasticity in palmierite-type$(1-x)Pb_3(PO_4)_{2-x}Pb_3(AsO_4)_2$. *Journal of Physics: Condensed Matter*, **29**, 213001.

Bosi F., Hatert F., Pasero M. and Mills S. (2023). Newsletter 73. *Mineralogical Magazine*, **87**, 639–643, https://doi:10.1180/mgm.2023.44

Cao R., Yu X., Sun X., Cao C. and Qiu J. (2014) Near-infrared emission $Ba_3(PO_4)_2:Mn^{5+}$ phosphor and potential application in vivo fluorescence imaging. *Spectrochimica Acta. Part A, Molecular and Biomolecular Spectroscopy*, **128**, 671–673.

Chance W. and Loye H.-C. zur. (2013) Synthesis, structure, and optical properties of a series of quaternary oxides, $K_2Ba(MO_4)_2$ (M = Cr, Mo, W). *Solid State Sciences*, **28**, 90–94.

Galuskina I.O., Galuskin E.V., Vapnik Y., Prusik K., Stasiak M., Dzierżanowski P. and Murashko M. (2017) Gurimite, $Ba_3(VO_4)_2$ and hexacelsian, $BaAl_2Si_2O_8$ – two new minerals from schorlomite-rich paralava of the Hatrurim Complex, Negev Desert, Israel. *Mineralogical Magazine*, **81**, 1009–1019.

García-Veigas J., Rosell L., Zak I., Playà E., Ayora C. and Starinsky A. (2009) Evidence of potash salt formation in the Pliocene Sedom Lagoon (Dead Sea Rift, Israel). *Chemical Geology*, **265**, 499–511.

García-Veigas J., Rosell L., Ortí F., Gündoğan İ. and Helvacı C. (2011) Mineralogy, diagenesis and hydrochemical evolution in a probertite–glauberite–halite saline lake (Miocene, Emet Basin, Turkey). *Chemical Geology*, **280**, 352–364.

Griniv S.P., Iorysh Z.I. and Skul'skaya L.I. (1986) Kalistrontite from the Stebnik deposit of potassium salts. *Mineralogicheskii Sbornik*, **40**, 74–78.

Grzechnik A. and McMillan P.F. (1997) High pressure behavior of $Sr_3(VO_4)_2$ and $Ba_3(VO_4)_2$. *Journal of Solid State Chemistry*, **132**, 156–162.

Juroszek R. and Ternes B. (2022) Crystal chemistry and Raman spectroscopy study of bennesherite, $Ba_2Fe^{2+}Si_2O_7$, and rare accessory Ba minerals from Caspar quarry, Bellerberg volcano, Germany. *Mineralogical Magazine*, **86**, 777–791.

Juroszek R., Galuskina I.O., Krüger B., Krüger H., Vapnik Y., Kahlenberg V., and Galuskin E.V. (2023) Minerals with a palmierite-type structure. Part I. Mazorite $Ba_3(PO_4)_2$, a new mineral from the Hatrurim Complex in Israel. *Mineralogical Magazine*, **87**, https://doi.org/10.1180/mgm.2023.56

Kemp S.J., Rushton J.C., Horstwood M.S.A. and Nénert G. (2018) Kalistrontite, its occurrence, structure, genesis, and significance for the evolution of potash deposits in North Yorkshire, U.K. *American Mineralogist*, **103**, 1136–1150.

Krzątała A., Krüger B., Galuskina I., Vapnik Y. and Galuskin E. (2020) Walstromite, $BaCa_2(Si_3O_9)$, from Rankinite Paralava within Gehlenite Hornfels of the Hatrurim Basin, Negev Desert, Israel. *Minerals*, **10**, 407.

Lacroix A. (1907) Sur une espèce minérale nouvelle des fumerolles à haute température de la récente éruption du Vésuve. *Comptes Rendus Hebdomadaires des Séances de l'Académie des Sciences*, **144**, 1397–1401.

Lagos C.C. (1970) Luminescence of Divalent Europium in Ba-Ca, Ba-Sr, and Ca-Sr Orthophosphate and Pyrophosphate Compositions. *Journal of The Electrochemical Society*, **117**, 1189–1193.

Maras A. (1979) Studi sui minerali del Lazio: la kalistrontite di Cesano. *Periodico di Mineralogia*, **48**, 195–203.

Mees F. (1999) Distribution patterns of gypsum and kalistrontite in a dry lake basin of the southwestern Kalahari (Omongwa pan, Namibia). *Earth Surface Processes and Landforms*, **24**, 731–744.

Merkle L., Pinto A., Verdún H. and McIntosh B. (1992) Laser action from Mn^{5+} in $Ba_3(VO_4)_2$. *Applied Physic Letters*, **61**, 2386–2388.

Mills S.J., Hatert F., Nickel E.H. and Ferraris G. (2009) The standardisation of mineral group hierarchies: application to recent nomenclature proposals. *European Journal of Mineralogy*, **21**, 1073–1080.

Min M. (1987) The first discovery of kalistrontite in China and its significance in search for potash deposits. *Acta Mineralogica Sinica*, **7**, 154–158.

Moore P.B. (1973) Bracelets and Pinwheels: A Topological-Geometrical Approach to the Calcium Orthosilicate and Alkali Sulfate Structures. *American Mineralogist*, **58**, 32–42.

Morris M.C., McMurdie H.F., Evans E.H., Paretzkin B., de Groot J.H., Newberry R., Hubbard C.R. and Carmel S.J. (1977) *Standard X-ray Diffraction Powder Patterns: Section 14. Data for 68 substances*. Report, Institute for Materials Research, National Bureau of Standards, Washington, DC.

Mu C. and He J. (2012) Synthesis and luminescent properties of Rare Earth (Eu^{2+}, Tb^{3+}) doped $Ba_3(PO_4)_2$ nanowires by chemical precipitation in nanochannels. *Materials Letters*, **70**, 101–104.

Mugavero S.J., Bharathy M., McAlum J. and zur Loye H.-C. (2008) Crystal growth of alkaline earth vanadates from hydroxide fluxes. *Solid State Sciences*, **10**, 370–376.

Murayama J.K., Nakai S., Kato M. and Kumazawa M. (1986) A dense polymorph of $Ca_3(PO_4)_2$: a high pressure phase of apatite decomposition and its geochemical significance. *Physics of the Earth and Planetary Interiors*, **44**, 293–303.

Pasero M., Kampf A.R., Ferraris C., Pekov I.V., Rakovan J. and White T.J. (2010) Nomenclature of the apatite supergroup minerals. *European Journal of Mineralogy*, **22**, 163–179.

Skelton R. and Walker A.M. (2017) Ab initio crystal structure and elasticity of tuite, γ-$Ca_3(PO_4)_2$, with implications for trace element partitioning in the lower mantle. *Contributions to Mineralogy and Petrology*, **172**, 87.

Smith A.L., de Zoete N., Rutten M., van Eijck L., Griveau J.-C. and Colineau E. (2020) Report of the double-molybdate phase $Cs_2Ba(MoO_4)_2$ with a palmierite structure and its thermodynamic characterization. *Inorganic Chemistry*, **59**, 13162–13173.

Sugiyama K. and Tokonami M. (1987) Structure and crystal chemistry of a dense polymorph of tricalcium phosphate $Ca_3(PO_4)_2$: A host to accommodate large lithophile elements in the Earth's mantle. *Physics and Chemistry of Minerals*, **15**, 125–130.

Sugiyama K. and Tokonami M. (1990) The crystal structure refinements of the strontium and barium orthophosphates. *Mineralogical Journal*, **15**, 141–146.

Süsse P. and Buerger M.J. (1970) The structure of $Ba_3(VO_4)_2$. *Zeitschrift für Kristallographie – Crystalline Materials*, **131**, 161–174.

Tāle I., Kūlis P. and Kronghauz V. (1979) Recombination luminescence mechanisms in $Ba_3(PO_4)_2$. *Journal of Luminescence*, **20**, 343–347.

Thompson R.M., Xie X., Zhai S., Downs R.T. and Yang H. (2013) A comparison of the $Ca_3(PO_4)_2$ and $CaSiO_3$ systems, with a new structure refinement of tuite synthesized at 15 GPa and 1300 °C. *American Mineralogist*, **98**, 1585–1592.

Tissot R.G., Rodriguez M.A., Sipola D.L. and Voigt J.A. (2001) X-ray powder diffraction study of synthetic Palmierite, $K_2Pb(SO_4)_2$. *Powder Diffraction*, **16**, 92–97.

Tong M., Liang Y., Yan P., Wang Q. and Li G. (2015) Synthesis and luminescence properties of a bluish-green emitting phosphor $Ba_3(PO_4)_2$: Ce^{3+}, Tb^{3+}. *Optics & Laser Technology*, **75**, 221–228.

Tsyrenova G.D., Pavlova E.T., Solodovnikov S.F., Popova N.N., Kardash T.Y., Stefanovich S.Y., Gudkova I.A., Solodovnikova Z.A. and Lazoryak B.I. (2016) New ferroelastic $K_2Sr(MoO_4)_2$: Synthesis, phase transitions, crystal and domain structures, ionic conductivity. *Journal of Solid State Chemistry*, **237**, 64–71.

Von Schwarz H. (1966) I. Sulfate. *Zeitschrift für Anorganische und Allgemeine Chemie*, **344**, 41–55.

Voronova M.L. (1962) Kalistrontite, a new mineral of potassium and strontium sulfate. *Zapiski Vserossiiskogo Mineralogicheskogo Obshchestva*, **91**, 712–717.

Xie X., Minitti M.E., Chen M., Mao H.K., Wang D., Shu J. and Fei Y. (2002) Natural high-pressure polymorph of merrillite in the shock veins of the Suizhou meteorite. *Geochimica et Cosmochimica Acta*, **66**, 2439–2444.

Xie X., Minitti M.E., Chen M., Mao H.-K., Wang D., Shu J. and Fei Y. (2004) Tuite, γ-$Ca_3(PO_4)_2$: a new mineral from the Suizhou L6 chondrite. *European Journal of Mineralogy*, **15**, 1001–1005.

Zachariasen W. (1948) The crystal structure of the normal orthophosphates of barium and strontium. *Acta Crystallographica*, **1**, 727–730.

Zambonini F. (1921) Sur la palmiérite du Vésuve et les mineraux qui l'accompagnent. *Comptes Rendus Hebdomadaires des Séances de l'Académie des Sciences*, **172**, 1419–1422.

Zelenski M.E., Zubkova N.V., Pekov I.V., Polekhovsky Y.S. and Pushcharovsky D.Y. (2012) Cupromolybdite, $Cu_3O(MoO_4)_2$, a new fumarolic mineral from the Tolbachik volcano, Kamchatka Peninsula, Russia. *European Journal of Mineralogy*, **24**, 749–757.

Zhai S., Yamazaki D., Xue W., Ye L., Xu C., Shan S., Ito E., Yoneda A., Yoshino T., Guo X., Shimojuku A., Tsujino N. and Funakoshi K.-I. (2013) P-V-T relations of γ-$Ca_3(PO_4)_2$ tuite determined by in situ X-ray diffraction in a large-volume high-pressure apparatus. *American Mineralogist*, **98**, 1811–1816.

https://doi.org/10.1180/mgm.2023.56 Published online by Cambridge University Press